J. Ocean Univ. China (Oceanic and Coastal Sea Research)
DOI 10.1007/s11802-014-2015-9
ISSN 1672-5182, 2014 13 (3): 347-355
http://www.ouc.edu.cn/xbywb/
E-mail:xbywb@ouc.edu.cn

Variability of Tropical Cyclone in High Frequent Occurrence Regions over the Western North Pacific

YANG Yuxing[1), 2), *], HUANG Fei[2)], and WANG Faming[1)]

1) *Institute of Oceanology*, *Chinese Academy of Science*, *Qingdao* 266071, *P. R. China*
2) *Department of Marine Meteorology*, *Physical Oceanography Laboratory and Key Laboratory of Ocean-Atmosphere Interaction and Climate in Universities of Shandong*, *Ocean University of China*, *Qingdao* 266100, *P. R. China*

(Received April 20, 2012; revised August 1, 2012; accepted March 12, 2013)

Abstract In this study, three high frequent occurrence regions of tropical cyclones (TCs), *i.e.*, the northern South China Sea (the region S), the south Philippine Sea (the region P) and the region east of Taiwan Island (the region E), are defined with frequency of TC's occurrence at each grid for a 45-year period (1965–2009), where the frequency of occurrence (FO) of TCs is triple the mean value of the whole western North Pacific. Over the region S, there are decreasing trends in the FO of TCs, the number of TCs' tracks going though this region and the number of TCs' genesis in this region. Over the region P, the FO and tracks demonstrate decadal variation with periods of 10–12 year, while over the region E, a significant 4–5 years' oscillation appears in both FO and tracks. It is demonstrated that the differences of TCs' variation in these three different regions are mainly caused by the variation of the Western Pacific Subtropical High (WPSH) at different time scales. The westward shift of WPSH is responsible for the northwesterly anomaly over the region S which inhibits westward TC movement into the region S. On the decadal timescale, the WPSH stretches northwestward because of the anomalous anticyclone over the northwestern part of the region P, and steers more TCs reaching the region P in the greater FO years of the region P. The retreating of the WPSH on the interannual time scale is the main reason for the FO's oscillation over the region E.

Key words high frequent occurrence regions; frequency of tropical cyclone's occurrence; western Pacific subtropical high

1 Introduction

It is well known that the tropical cyclone (TC) is one of the most devastating natural disasters, especially in most frequent TC regions. Over the Western North Pacific (WNP), which is one of the most frequent TC regions, climatological variations of TC activities have been studied in literature (*e.g.*, Chia and Ropelewski, 2002; Wang and Chan, 2002; Wu and Wang, 2004; Leung *et al.*, 2005; Wang *et al.*, 2006; Goh and Chan, 2010; Kim *et al.*, 2010; Choi and Byun, 2010; Wang *et al.*, 2010). For the formation and movement of TCs, Gray (1968, 1979) identified six factors as the basic conditions of TCs generation, which are the Coriolis parameter, low-level vorticity at 850 hPa, vertical shear of zonal wind, sea surface temperature, mid-level moisture, and moist instability of low-to-mid troposphere. Chia and Ropelewski (2002) and Wang *et al.* (2007) suggested that vorticity related to the monsoon trough at 850 hPa and strong outflow caused by divergence at 200 hPa (Yumoto and Matsuura, 2001) are also important for TCs building up. Fu *et al.* (2012) indicated that the 800 hPa maximum relative vorticity, rain rate, vertically averaged horizontal shear, vertically averaged divergence and 925–400 hPa water vapor content are important to the TC genesis in the WNP. For the movement of TCs, previous researchers pointed out that the flow between 850–300 hPa can act as a steering flow of TCs (Holland, 1993, Wu *et al.*, 2005), which is further influenced by the Western Pacific Subtropical High (Ho *et al.*, 2004; Lee *et al.*, 2006).

For the variation of TC activities over the whole WNP, literatures show that there are interannual variation associated with the El Niño-Southern Oscillation (ENSO; Chen *et al.*, 1998; Wang and Chan, 2002; Hong *et al.*, 2011; *etc.*), and long term trend associated with global warming (*e.g.*, Webster *et al.*, 2005, 2006; Emanuel, 2005; Wu and Wang, 2004; Landsea *et al.*, 2006; Klotzbach, 2006). Also, the TCs' variations at sub-regions of the WNP are studied (Ho *et al.*, 2004; Wu *et al.*, 2005; Li and Duan, 2010). Ho *et al.* (2004) did researches about typhoon track changes in the two periods (1951–1979 and 1980–2001) and pointed out that different sub-regions experience different changing trend of typhoon's frequency. Their results suggest that there are significantly decreasing typhoon frequency (the percentage values of the total number of typhoon passage into a 5°×5° latitude-longitude grid box with respect to the total number

* Corresponding author. Tel: 0086-532-82898933
E-mail: yangyx@qdio.ac.cn

of typhoons formed in the WNP) in the East China Sea and Philippine Sea, but slightly increasing typhoon frequency in the South China Sea (5°–15°N, 110°–125°E). The results of Wu *et al.* (2005) show that the subtropical East Asia has experienced increasing typhoon influence, but the number of typhoons over the South China Sea is considerably decreased from 1965 to 2003 because of the westward shift of typhoon track. Kubota and Chan (2009) studied the TCs which land on the Philippine region and found that the interdecadal variability of TC landfall number in the Philippines is related to different phases of ENSO and Pacific Decadal Oscillation. Comparing to previous study of TC activities over the whole WNP basin, this paper focuses on the regions where the TCs are more active and more intense. Within the WNP, variations of TCs over three high frequent occurrence regions (HFOR) of TCs are dominant at different time scales. And it is shown that the variations of TCs at those regions are strongly related to the variation of background circulation at different time scales.

The paper is arranged into five sections. Data and methods are described in Section 2, together with the definition of HFOR. The variability of TCs over the three HFORs is analyzed separately in Section 3. Section 4 elucidates the relationship between TCs' variability over HFORs and background circulation. The last section presents summary and discussion.

2 Data and Methods

Best-track datasets of TCs during the period 1965–2009 from the Joint Typhoon Warning Center are used (http://www.usno.navy.mil/NOOC/nmfc-ph/RSS/jtwc/best_tracks). The reason for choosing this period is that since 1965 the satellite monitoring of weather events first becomes routine and, as a result, no TC would be missed within the chosen period. The TCs with intensity reaching tropical storm (wind speed $\geq 17 \mathrm{m\,s^{-1}}$) are considered. In the paper, the frequency of occurrence (FO) indicates how many TCs enter a grid box of 2.5° latitude by 2.5° longitudes and how long TCs stay in this grid box.

To better understand the relationship between the circulation and the variability of TC activities, winds, geopotential height, relative humidity and sea surface temperature (SST) are analyzed from the National Centers for Environmental Prediction-National Center for Atmospheric Research (NCEP-NCAR) reanalysis data (www.cdc.noaa.gov/cdc/reanalysis) during the same period of 1965–2009. These datasets are on regular grids with a horizontal resolution of 2.5°×2.5° for atmospheric variable and 2.0°×2.0° for SST. The Pacific Decadal Oscillation (PDO) index is offered by the Nate Mantua (Zhang *et al.*, 1997; Mantua *et al.*, 1997).

It is found that more than 1/3 of all TCs activities over whole WNP during the 45 years appear in the highlighted region in Fig.1 (red in color). The HFOR of TCs is defined with a criterion that a value of the FO in each grid box (over 155) is triple the mean value of FO over the whole WNP basin. Further analysis shows that the TC activity has different features in the HFOR at the north part of the South China Sea, southern Philippine Sea and the east of the Taiwan Island. The three HFORs are defined as the region S (the north part of the South China Sea), the region P (the southern Philippine Sea) and the region E (the East of the Taiwan Island) respectively (Fig.1). The boundary between the region S and P is 121.25°E, and that between the region E and P is 21.25°N (shown with black lines in Fig.1).

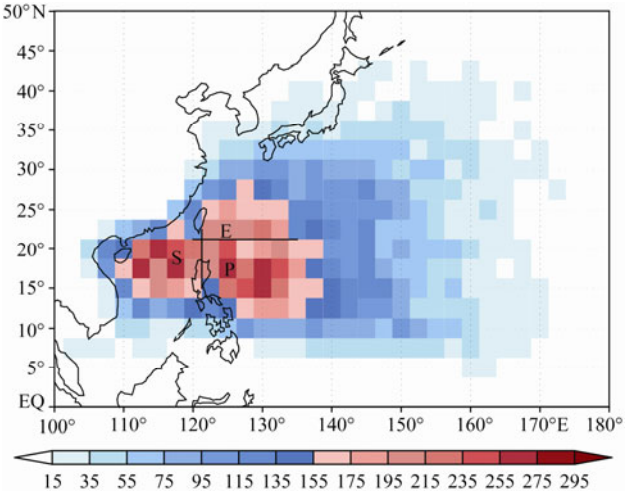

Fig.1 The distribution of the total FO of the TCs of the period 1965–2009, and the three HFORs: region S, region P and region E.

3 Variability of TCs' FO in Three HFORs

To express the variability of FO over the three HFORs, the total FO index in each HFOR is calculated. Fig.2 shows the climatological seasonal cycle of TCs' FO indices over the three HFORs. It is easy to find that seasonal variation in the region P shows a bimodal mode, with two peaks at July and October. Over the region P, the FO is about 19 in October and 16 in July. The variations in re-

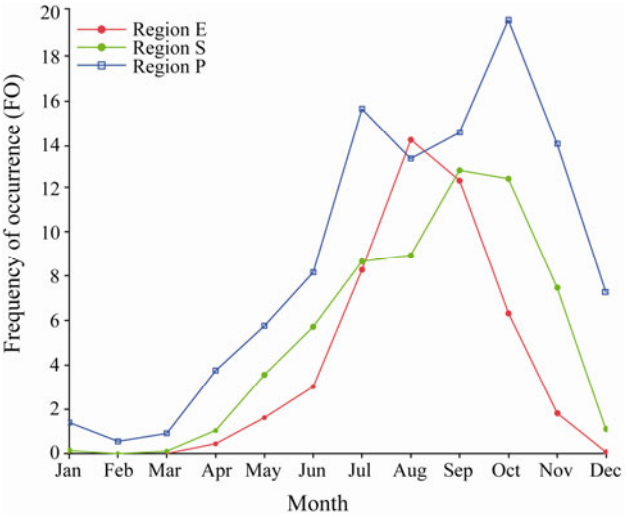

Fig.2 The seasonal variability of the climatological mean FO of region E (red line), region S (green line), and region P (blue line).

gions E and S only have one peak, which is smaller than 15. The FO shows a maximum of 14 at August for the region E and a peak value of 13 at September for the region S (Fig.2). Although there are differences in the occurrence of maximum FO at different regions, all maximum fall into typhoon peak season (July to November, JASON). Based on this seasonal distribution of TCs' FO, the following analysis will focus on the peak season (JASON) of TCs.

Fig.3 shows interannual variation of FO summed in JASON at three HFORs from 1965 to 2009. Over the region S, the FO of TCs shows clear downward trend, which passes the 99% confidence level (shown with green line in Fig.3a). There is no significant interannual or decadal variation in this time series (shown in Fig.4a). Over the region P, the variation of TCs' FO demonstrates an about 12 years decadal variation and an around 30 years interdecadal variation above the 95% confidence level (shown in Fig.4b). Over the region E, there is neither a significant trend nor an interdecade variability of FO during this 45-year period. But based on wavelet analysis (shown in Fig.4c), an around 4 years' oscillation of FO passing the 95% significance test exists at the region E.

As we know that the FO is strongly influenced by the genesis as well as the track of TCs. TCs' track number (TN) and TCs' genesis number (GN) are next discussed. The TN is defined as the total number of TC passages into a region, and the GN expresses the number of TCs formed in a subregion. Therefore, the variability of the TN (Figs.3b, 3e, 3h) and GN (Figs.3c, 3f, 3i) in three HFORs are also investigated. In the region S (Figs.3a, 3b, 3c), all indices, including FO, TN and GN, show significant decreasing trends (shown with dash lines in Fig.3). This means that the downward trend of FO in the region S is related to the decreasing of TC passing through this region and the TC genesis in this region. The variations of FO, TN and GN over the region P (Figs.3d, 3e, 3f) all exhibit significant decadal and interdecadal oscillations in wavelet analysis (figures not shown). The correlation coefficient between FO and TN is 0.552, far exceeding 99% confidence level, while the correlation coefficient between FO and GN is only 0.281. From the 9 years running mean (thick lines in Figs.3d, 3e, 3f), the correlation coefficients are 0.811 between FO and TN, but only 0.347 between FO and GN. This suggests that the FO of TCs is mainly influenced by TN, especially at decadal and interdecadal time scale. The variability of FO and TN in the region E displays clearly periods of 4–5 years (Figs.3g, 3h). Time series of FO over the region E show similar variation to that of TN, with the correlation coefficient between them reaching 0.65. Due to the location of the region E, very few TC geneses are over this region. Hence, there is no obvious period for GN in the region E (Fig.3i). As a result, the correlation coefficient between FO and GN is only 0.05 for this region. Therefore, similar to region P, the variation of FO in the region E is mostly influenced by the track of TCs passing through this region.

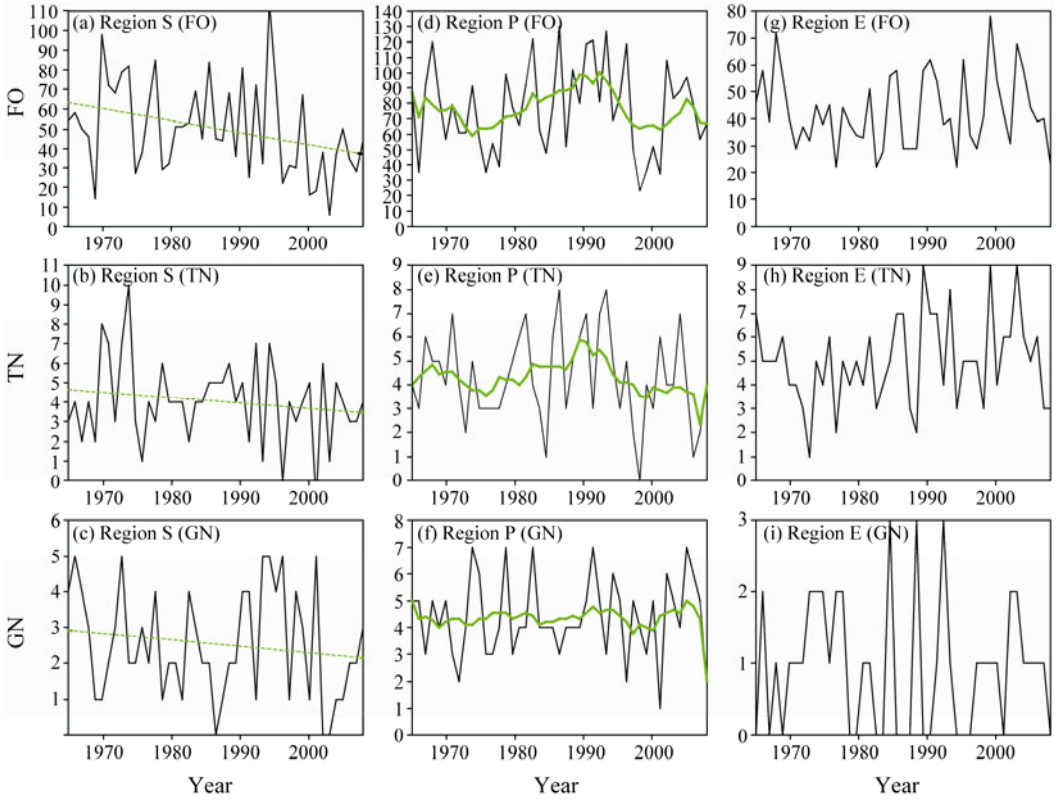

Fig.3 The time series of the July, August, September, October and November (JASON) summed FO (a, d, g), TN (b, e, h), and GN (c, f, i) in the regions S (a, b, c), P (d, e, f), and E (g, h, i). The dashed lines in (a, b, c) denote the linear slope for the entire period (1965–2009), while the thick lines (d, e, f) represent the result of the 9-points smooth data of the FO, TN and GN of the region P.

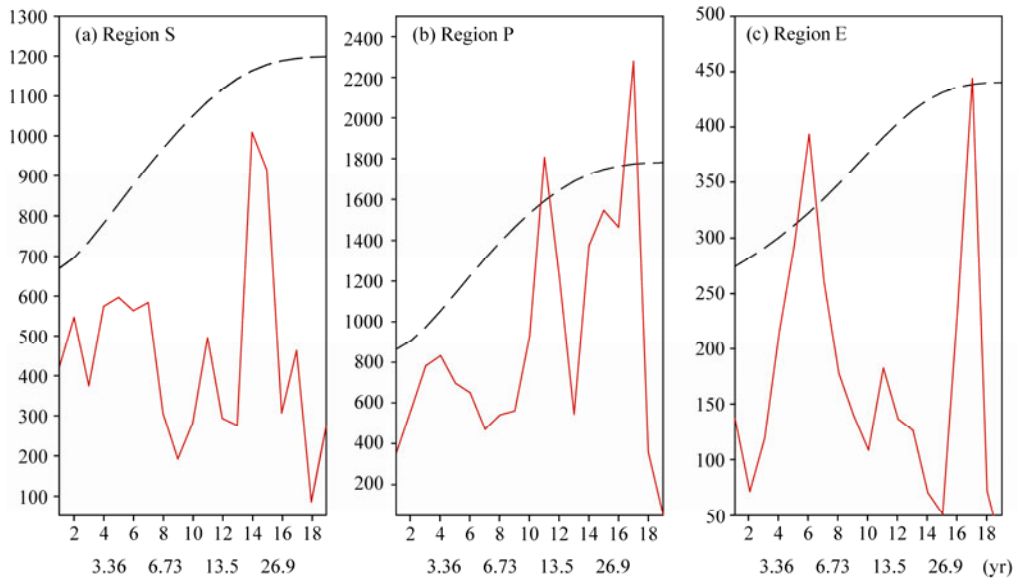

Fig.4 The global wavelet spectrum of the TC FO in the three regions (a-region S, b-region P, and c-region E), in which the dashed line is the 95% confidence level and the numbers at the bottom of the figure are the periods (unit: year).

4 Large Scale Environmental Factors

4.1 The Effects of Environment Factors on the Trend in the Region S

In the above discussion, we show that there is a decreasing trend in FO, TN and GN over the region S (Figs.3a, 3b, 3c). The decreasing trend of the FO over the region S may be a result of downward trends of TCs genesis in this region and TCs' tracks through the region. To better understand what causes the decreasing trend, the relationship between those indices at the region S and the background circulation is analyzed.

Since there is a similar linear decreasing trend, we simply divide the 45 years into two time periods and compare their means of magnitudes of some items. The first one is from 1965 to 1986, called the earlier period. The second one is from 1987 to 2009, named the later period. The variation of tracks though the region S is in turn affected by changes in large-scale air steering flows. We use mean flows between 850–300 hPa to indicate steering flows (Holland, 1993 and Wu *et al.*, 2005), and analyze changes of the mean flows for the two sub-periods to discuss the movement of TCs. Meanwhile, we compare the climatological mean TC translation vectors between the earlier period and later period. The mean TC translation vectors are calculated at each 2.5°×2.5° grid box based on all the TCs that pass across each box. Fig.5a represents the differences of JASON mean translation vectors, while Fig.5b shows SST and the mean steering flows between the two periods. From Fig.5a it can be found that the change of the translation vector between the two periods shows reduced westward tracks in the region S, the anomalies of the translation vector over the region S in the later period is eastward, and this is consistent with the results of Wu *et al.* (2005). In the southwestern region of the region S (around 10°N), the change of the mean motion is westward, and the FO has positive anomaly. This result agrees well with Zuki and Lupo (2008) which indicates that there is a slightly increasing trend in TC activity in the southern South China Sea region.

The changes in the mean TC translation velocity in these two regions (Fig.5a) are closely associated with the large-scale steering flow. As shown in Fig.5b, SST in the second period displays significant positive anomaly in the WNP, especially along the coast regions (including the region S). The isopotential contours of geopotential high in Fig.5b indicate the westward shift of the Western Pacific Subtropical High (WPSH) during the later period (blue ones). The width of WPSH is larger in the period 1987–2009 (blue contours in Fig.5b) than that in the earlier period (green contours in Fig.5b). Meanwhile, during the later period, the change of the wind vectors shows cyclonic circulation over the east China and anti-cyclonic circulation over the South China. The region S locates in the south part of the cyclonic circulation and the north part of the anti-cyclonic circulation, so the significant northwesterly wind is over the region S and the westward steering flows appear around the southwest of the region S. So we try to give such a hypothesis: the westward shift of WPSH is responsible for the anti-cyclonic flow anomaly over the South China Sea. This shift, in turn, cause the northwesterly anomaly over the region S, resulting in inhibiting the westward TC movement into the region S. On the other hand, the westward shift of WPSH also induces easterly flow anomaly over the southern South China Sea, resulting in the increase in TC tracks over the region. The contours in Fig.5c show the departures of mean geopotential height of 850–300 hPa which are computed as the differences from global mean for the later and earlier periods (Murakami *et al.*, 2011). As shown by comparing the two periods, the location of the WPSH has no significant variation, which suggests that global warming may play an important role in the westward shift of the WPSH.

For the decreasing trend of the FO, another important factor is the variation of the genesis in the region S. As shown in Fig.3c, the decreasing trend of GN in region S is significant at the 90% confidence level. The change of the genesis is mainly affected by the change of thermodynamic and hydrodynamic factors, such as SST, low-level relative humidity, low-level vorticity, vertical wind shear, *etc.* The study of the Fu *et al.* (2012) indicates that in the WNP the 800 hPa maximum relative vorticity, vertically averaged horizontal shear, vertically averaged divergence and 925–400 hPa water vapor content are important for the disturbances developing into TCs. In this paper, we discuss all the factors mentioned above and show the significant changes in Fig.6. This figure depicts the difference of the influencing factors between the two periods (magnitude of a farter in the later period minus that in the earlier period). The results show that changes of most circulation factors in the two period over the region S are not favorable for TC to develop in this region except for the decreasing of the vertically averaged divergence (Fig.6e) and warmer SST (Fig.5b). In the region S, the relative humidity at 850 hPa during the later period is significantly lower than that in the earlier period (Fig.6a). And vertically averaged horizontal shear shows significant positive anomaly over the region S (Fig.6d). The increased vertical shear (Fig.6c), weakened relative vorticity at 800 hPa (Fig.6c) and decreased water vapor content (Fig.6f) over the region S are also not favorable for TC genesis, but the resulting changes are not significant. Chan (2009) indicated that thermo-dynamic factors are not important for TC genesis over the WNP, which may mean that the change of the vertically averaged horizontal shear can be responsible for the decreasing tend of the TC genesis in the region S.

4.2 The Relationship Between General Circulation and Decadal Variation in the Region P

As mentioned above, the variation of FO in the region P shows significant decadal (around 10–12 years) and interdecadal oscillations (around 30 years). Because a 45-year data set is too short for a 30-year oscillation, the following analysis focuses on the decadal variation. The 9-years smoothed data of FO, TN and GN are used to show the decadal oscillation (the green lines in Fig.3). The decadal variation result in high covariance between the 9-points smoothed curve of FO and that of TN, with the correlation coefficient reaching 0.81. This indicates that the decadal variation of the FO is mainly due to the variability of the TN. So the following analysis focuses on the influence of general circulation on the TN.

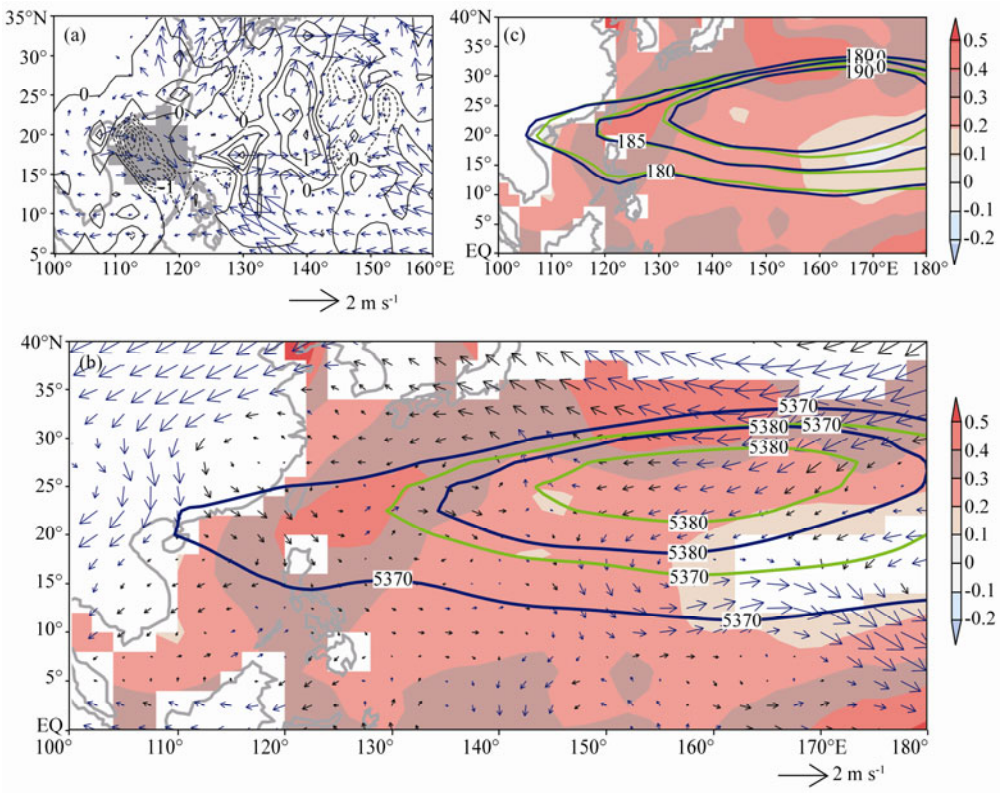

Fig.5 (a) Difference of the July–November mean FO (contours) and the motion vectors (vectors) between the period 1987–2009 and 1965–1986, in which the grey shade denotes the region S; (b) the differences of JASON mean SST (shaded, ℃, which is over the confidence level 90% of *t*-test) and mean steering flows of 850–300hPa (vectors), in which the blue and green contours are geopotential height for the period 1987–2009 and 1965–1986, respectively, and the blue vectors means the vector over the confidence level 90% of *t*-test; (c) the differences of JASON mean SST (shaded, ℃) and the departures of mean geopotential height of 850–300 hPa (colored contours, gpm), in which the departure of geopotential height is computed as the difference from global mean for 1987–2009 (blue contours) and 1965–1986 (green contours).

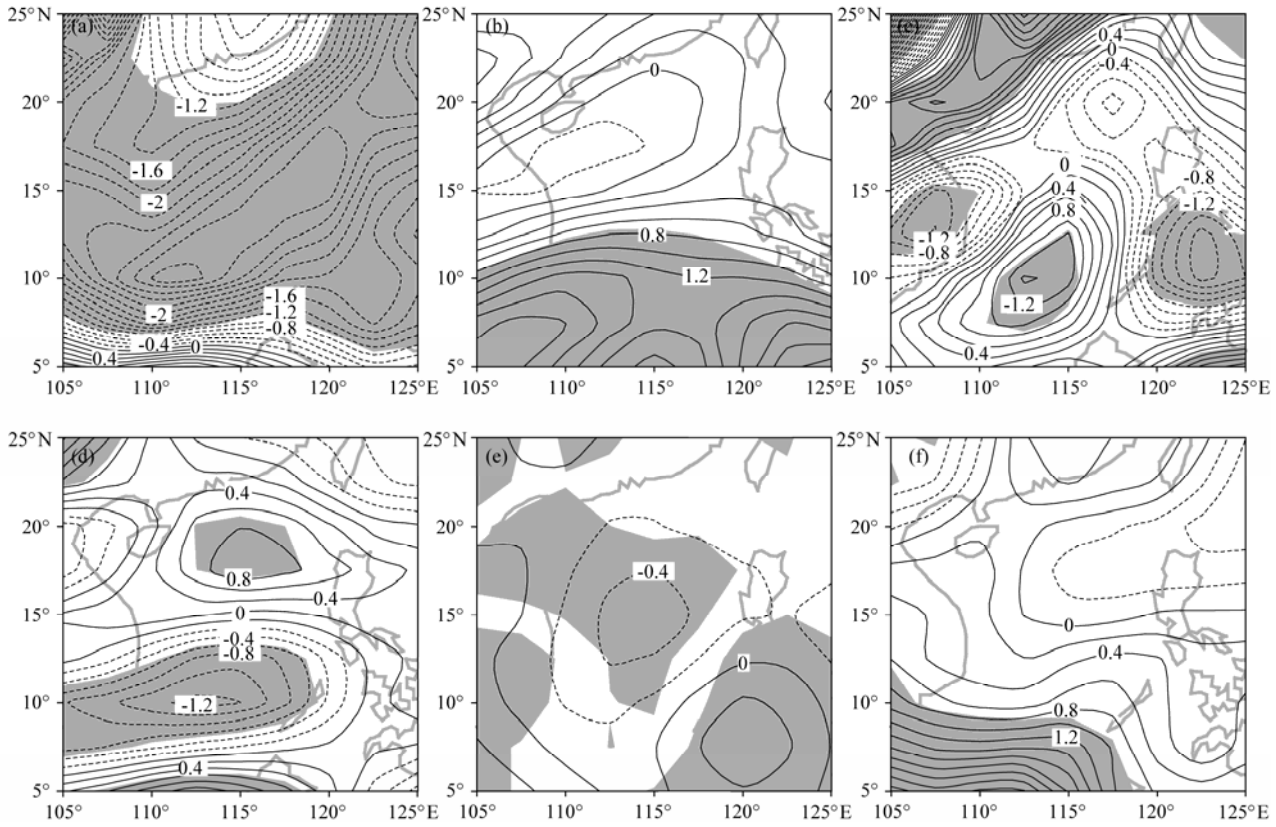

Fig.6 The geographical distribution of the differences of the circulation factors between 1987–2009 and 1965–1986. (a) the relative humidity (%) at 850 hPa, (b) the vertical shear ($m\,s^{-1}$), (c) 800 hPa relative vorticity ($10^{-6}\,s^{-1}$), (d) vertically average zonal shear $\partial u/\partial y$ ($10^{-6}\,s^{-1}$), (e) vertically averaged divergence ($10^{-6}\,s^{-1}$) and (f) 925–400 hPa water vaper ($g\,kg^{-1}$) (shaded, which is over the confidence level 90% of *t*-test; contours, interval=0.4).

Based on the normalized 9-points smoothed curve of FO, twelve greater FO years (standard deviation is greater than 0.75) and fourteen smaller FO years (standard deviation is less than −0.75) are defined. The greater FO years are 1965, 1983, 1986, 1987, 1988, 1989, 1990, 1991, 1992, 1993, 1994, and 1995, which mainly concentrate in mid 1980s and early 1990s. On the other hand, the smaller FO years mostly appear in the 1970s and early 21st century, *i.e.*, 1973, 1974, 1975, 1976, 1977, 1978, 1998, 1999, 2000, 2001, 2002, 2003, 2008, and 2009. Based on the definition of the two FO regimes, composite analysis is used to identify the differences between the greater and smaller FO years.

Fig.7 shows the difference of translation vectors, SST and steering flows between the greater and smaller FO years. The variation of the translation vectors is consistent with that of the steering flow, especially in the region P. In this region (shown in Fig.7, those in the higher FO years minus those in the lower FO years), the difference of the translation vectors between the higher FO years and lower FO years is westward, meaning that the westward tracks will increase and the northwest tracks will be reduced in the higher FO years. This agrees well with the steering flow as shown in Fig.7c. The composite result of the mean flows (850–300 hPa) shows an anticyclone on the north of the region P (form 100˚E to 140˚E), and the westward wind of this anticyclone appears just in the region P. And this anticyclone makes the WPSH stretch westward. The geopotential height (850–300 hPa) which is subtracted from the global mean height in the higher FO years clearly extends westward (red contours in Fig.7c). It is favorable for the westward tracks going through the region P. This composite analysis shows the influence of difference between the general circulation in the 1980s and early 1990s and that in the 1970s and early 21st century, which is the result of the decadal variation of the general circulation. Previous studies indicated that there is significant interdecadal variation in the late 1970s (Ho *et al.*, 2004) and the 1990s (Sui *et al.*, 2007; Wu and Zhou, 2008). So it may mean that the interdecadal variation of the WPSH plays a key role in the decadal variation of FO over the region P. Further analysis of this decadal variation shows that it is related to the PDO. As shown in Fig.7c the SST anomaly pattern displays the PDO structure, and the higher and lower FO years are corresponding to the positive and negative phase respectively (Fig.7b). The correlation coefficient 0.346 between the FO in region P and the index of PDO is significant at the 95% confidence level.

In addition, the translation vectors and mean flows do not match so well in the WNP except for region P, especially in the south of the region P (5˚–10˚N) and the east of the region P (140˚–150˚E). That may be because the composite results are based on the variation of the region P, and in other places the FO of TCs do not show the same variation as that of the region P.

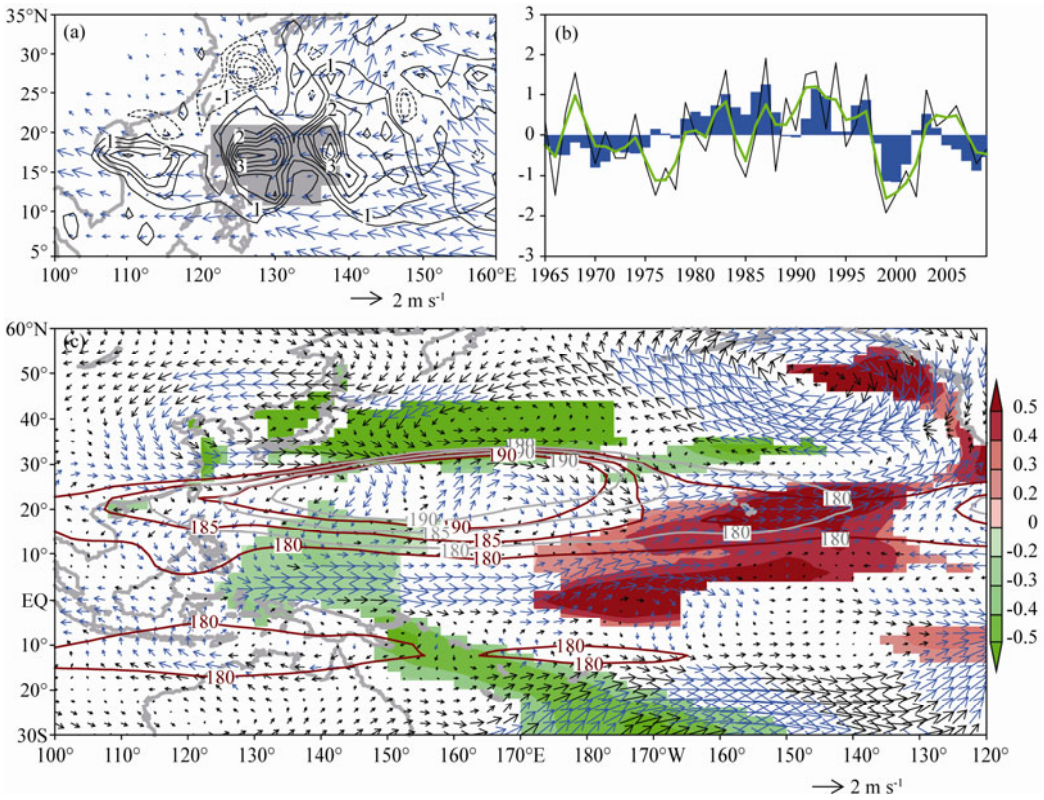

Fig.7 (a) Difference of the July–November mean FO (contours) and the motion vectors (vectors) between higher FO years and lower FO years based on the normalized results of 9-point smooth FO time series of the region P (the standard deviation larger than 0.75 defines higher FO year, while the standard deviation less than −0.75 defines lower FO year), in which the grey shadow denotes the region P; (b) The normalized time series of JASON FO (black line) in the regions P, 9-year running mean of the black line (green line), and the 9-year running mean of PDO index (blue bar); (c) The differences of JASON mean SST (shaded, ℃), mean steering flows of 850–300 hPa (vectors) between higher FO years and lower FO years and departures of mean geopotential height of 850–300 hPa (colored contours, gpm). The blue vectors means the vector over the confidence level 90% of *t*-test; the departure of geopotential height is computed as the difference from global mean for higher FO years (red contours) and lower FO years (grey contours).

4.3 The Relationship Between General Circulation and Interannual Variation in the Region E

Similar to the previous analysis of decadal variation in the region P, the interannual variability in the region E is also studied by compositing analysis of two different groups. It is shown in the previous discussion that the FO's variation in the region E is influenced by the variability of TN. Therefore, using the standard deviation as a criterion, two groups of FO years are chosen, *i.e.*, the thirteen greater FO years (1966, 1968, 1969, 1985, 1986, 1990, 1991, 1992, 1996, 2000, 2001, 2004, 2005) with standard deviation greater than 0.75 and the thirteen smaller FO years (1971, 1973, 1977, 1981, 1983, 1984, 1987, 1988, 1989, 1995, 1998, 2003, 2009) with standard deviation less than −0.75.

Here we also give results of difference of the translation vectors and the steering flows between the two FO groups (shown in Fig.8, those in the higher FO years minus those in the lower FO years). Over the region E, the difference of the translation vectors are main westward ones, consistent with those over the east region of the region E. In the south region of the region E, the difference of the translation vectors show eastward. From Fig.8a, it can be found that compared with the lower FO years, in the higher FO years the westward tracks are reduced, while the northwest and recurving tracks increase. It may result from the variation of the steering flows. Over and around the region E, SST anomaly shows negative difference, with wind and geopotential height field displaying a cyclonic circulation (Fig.8b). On the other hand, there is a positive SST anomaly at the southeastern WNP. Companied to the SST anomaly, an anomalous wind field follows anti-cyclonic circulation at the southeastern WNP. These anomalous circulations will weaken the northwest part of WSPH and strengthen the southeast part of it. It indicates that the WPSH would retreat southeastward during the greater FO years. It is well known that retreat of the WSPH provides a favorable condition for more northwest moving or recurving tracks of TCs occurring over the WNP. Because the TCs coming through the region E are mostly northwest moving TCs, this variation of WPSH in the greater FO years contributes to the increase of number of TCs passing through the region E. It infers that the interannual variation of the WSPH is the main reason of the variability for FO in the region E.

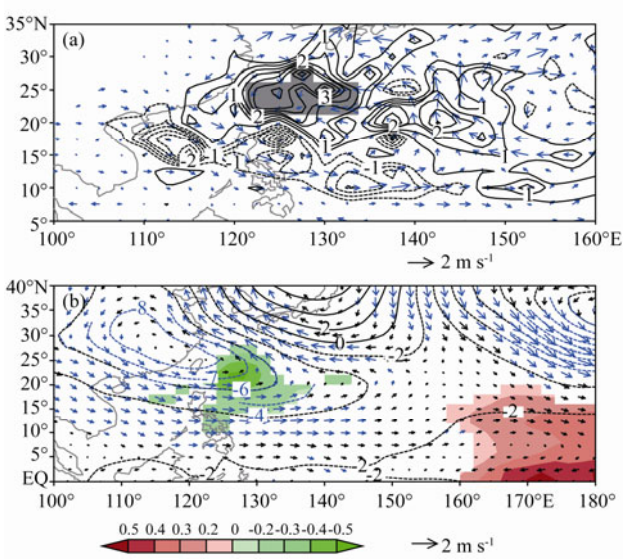

Fig.8 (a) Difference of the July-November mean FO (contours) and the motion vectors (vectors) between higher FO years and lower FO years based on the normalized time series of FO of the region E (the standard deviation larger than 0.75 defines larger FO year, while the standard deviation less than −0.75 defines smaller FO year), in which the grey shadow denotes the region E; (b) The differences of JASON mean SST (shaded, ℃), mean steering flows of 850–300 hPa (vectors) and geopotential height (contour) between higher FO years and lower FO years. The blue vectors and the blue contours mean result with over confidence level 90% of *t*-test (in b).

5 Summary and Discussion

Based on the 45-year (1965–2009) TC data, some new results on variation of TC activities are presented in this paper. Because there are more than 75% of TC activities in the peak season (JASON), the discussions of TC activity in our paper focus on the peak season over three regions. First, a very useful definition of the HFOR is given as the region where the FO is triple the mean value of the whole WNP. In those regions, TCs are more active, indicating that the number of TCs that come through the region is larger or the time they stay there is longer. Based on such definition, three HFORs over the WNP are found, *i.e.*, the northern South China Sea (the region S), the south Philippine Sea (the region P) and the region east of Taiwan Island (the region E). Over the region S, there are significant decreasing trends of FO, TN and GN of TCs in JASON. Over the region P, the corresponding indices in JASON show about 10–12 years decadal variations with over 95% confidence level. Over the region E, neither significant long term trend, nor decadal variation exists for FO. But there is an obvious around 4 years interannual oscillation of FO over the region E. The FOs of three HFORs are discussed together with the two influence factors, TN and GN. It is shown that for all three regions the TN's variability is a main contributor to the FO's variation. For the region S, the change of GN is another factor in the long-term trend of FO.

For the variation of the TC in the South China Sea, the region east of the Taiwan Island and the region around the Philippines, there have been some published works, in which the researchers separate the target areas mainly based on their locations. But we defined the three HFORs based on the TC activities and the locations. For the deceasing trend of the region S, Wu *et al.* (2005) indicated that this decreasing trend resulted from the two prevailing typhoon tracks shifting westward. In this paper, we give another interpretation. Because of global warming, the WPSH widens, stretching westward and making the region S covered by an anticyclone. So the northwesterly steering flows are against the westward track going through the region S, and the westward steering flows shift to the southern of the region S, which may cause the TC number to increase in the southern South China Sea (Zuki and Lupo, 2008) and decrease in the region S.

The decadal variation of the FO in the region P has a close relationship with the interdecadal change of the WPSH. As in previous studies, there is significant interdecadal variation in the late 1970s (Ho *et al.*, 2004) and in the 1990s (Sui *et al.*, 2007; Wu and Zhou, 2008; Zhou *et al.*, 2009); the FO in the region P shows lower FO in the 1970s and early 21st century, while in 1980s and early 1990s it is higher. The decadal variation of WPSH stretches westward, the westward steering flows control the region P, and the westward tracks coming through the region P result in a higher FO. Further analysis shows that this decadal variation may be related to the PDO, with a correlation coefficient 0.346 between the FO in JASON and PDO index.

The interannul variation of the FO in region E is related to the interannual variation of the WPSH. In the higher FO years, the WPSH shows an eastward and southward retreat, and more northwestward travelling or revurving TCs can go through the region E. Tu *et al.* (2009) indicated that there is an abrupt change of the TC number in the region E (from June to October) in 2000 based on the data of 1970–2005; but in our study we find that after 2005 the number decreases to the level before 2000. So there is no significant shift of TN in the region E from 1965 to 2009.

Acknowledgements

The work was supported by the National Natural Science Foundation of China (Nos. 41106018, 40975038) and Program 973 (Nos. 2012CB417402, 2010CB950402, 2012CB955604).

References

Chan, J. C. L., 2009. Thermodynamic control on the climate of intense tropical cyclones. *Proceedings of the Royal Society A*, **465**: 3011-3022.

Chen, T. C., Weng, S. P., Yamazaki, N., and Kiehne, S., 1998. Internanual variation in the tropical cyclone formation over the Western North Pacific. *Monthly Weather Review*, **126**: 1080-1090.

Chia, H. H., and Ropelewski, C. F., 2002. The interannual variability in the genesis location of tropical cyclones in the northwest Pacific. *Journal of Climate*, **15**: 2934-2944.

Choi, K. S., and Byun, H. R., 2010. Possible relationship between North Pacific tropical cyclone activity and Arctic Oscillation. *Theoretical and Applied Climatology*, **100**: 261-274.

Emanuel, K. A., 2005. Increasing destructiveness of tropical cyclones over the past 30 years. *Nature*, **436**: 686-688.

Fu, B., Peng, M. S., Li, T., and Stevens, D. E., 2012. Developing versus non-developing disturbances for tropical cyclone formation part II: Western North Pacific. *Monthly Weather Review*, **140**: 1067-1080.

Goh, A. Z. C., and Chan, J. C. L., 2010. Interannual and interdecadal variation of tropical cyclone in the South China Sea. *International Journal of Climatology*, **30**: 827-843.

Gray, W. M., 1968. Global view of the origin of tropical disturbances and storms. *Monthly Weather Review*, **96**: 669-700.

Gray, W. M., 1979. Hurricanes: Their formation, structure and likely role in the tropical circulation. In: *Meteorology Over Tropical Oceans*. Shaw, D. B., ed., Royal Meteorological Society, RG12 1BX, 155-218.

Ho, C. H., Baik, J. J., Kim, J. H., Gong, D. Y., and Sui, C. H., 2004. Interdecadal changes in summertime typhoon tracks. *Journal of Climate*, **17**: 1767-1776.

Holland, G. J., 1993. Tropical cyclone motion. In: *Global Guide to Tropical Cyclone Forecasting*. World Meteorological Organization Tech. Document WMO/TD 560, Tropical Cyclone Programme Rep. TCP-31, Chapter 3, Geneva, Switzerland.

Hong, C. C., Li, Y. Y., Li, T., and Lee, M. Y., 2011. Impacts of central Pacific and eastern Pacific El Niños on tropical cyclone tracks over the western North Pacific. *Geophysical Research Letters*, **38**: L16712.

Kim, J. H., Ho, C. H., and Chu, P. S., 2010. Dipolar redistribution of summertime tropical cyclone genesis between the Philippine Sea and the northern South China Sea and its possible mechanisms. *Journal of Geophysical Research*, **115**, D06104, DOI: 10.1029/2009JD012196.

Klotzbach, P. J., 2006. Trends in global tropical cyclone activity over the past twenty years (1986–2005). *Geophysical Research Letters*, **33**, L10805, DOI: 10.1029/2006GL025881.

Kubota, H., and Chan, J. C. L., 2009. Interdecadal variability of tropical cyclone landfall in the Philippines from 1902 to 2005. *Geophysical Research Letters*, **36**, L12802, DOI: 10.1029/2009GL038108.

Landsea, C. W., Harper, B. A., Hoarau, K., and Knaff, J. A., 2006. Can we detect trends in extreme tropical cyclones? *Science*, **313**: 452-454.

Lee, C. S., Lin, Y. L., and Cheung, K. K. W., 2006. Tropical cyclone formations in the South China Sea associated with the Mei-yu front. *Monthly Weather Review*, **134**: 2670-2687.

Leung, Y. K., Wu, M. C., and Chang, W. L., 2005. Variation of tropical cyclone activity in the South China Sea. Presented in ESCAP/WMO Typhoon Committee Annual Reciew 2005, November 2006, Hong Kong Observatory Reprint, No. 675.

Li, Q., and Duan, Y., 2010. Tropical cyclone strikes at the coastal cities of China from 1949 to 2008. *Meteorology and Atmospheric Physics*, **107**: 1-7.

Mantua, N. J., Hare, S. R., Wallace, J. M., and Francis, R. C., 1997: A Pacific decadal climate oscillation with impacts on salmon production. *Bulletin of the American Meteorological Society*, **78**: 1069-1079.

Murakami, H., Wang, B., and Kitoh, A., 2011. Future change of western North Pacific thphoons: Projections by a 20-km-mesh global atmospheric model. *Journal of Climate*, **24**: 1154-1169.

Sui, C. H., Chung, P. H., and Li, T., 2007. Interannual and interdecadal variability of the summertime western North Pacific subtropical high. *Geophysical Research Letters*, **34**, L11701.

Tu, J. Y., Chou, C., and Chu, P. S., 2009. The abrupt shift of typhoon activity in the vicinity of Taiwan and its association with western North Pacific-East Asian climate change. *Journal of Climate*, **22**: 3617-3628.

Wang, B., and Chan, J. C. L., 2002. How strong ENSO events affect tropical storm activity over the western North Pacific? *Journal of Climate*, **15**: 1643-1658.

Wang, B., Yang, Y. X., Ding, Q. H., Mueakami, H., and Huang, F., 2010. Climate control of the global tropical storm days (1965–2008). *Geophysical Research Letters*, **37**, L07704, DOI: 10.1029/2010GL042487.

Wang, H., Ding, Y., and He, J., 2006. Influence of western north Pacific summer monsoon changes on typhoon genesis. *Acta Meteorologica Sinica*, **64**: 345-356.

Wang, L., Lau, K.-H., Fung, C. H., and Gan, J. P., 2007. The relative vorticity of ocean surface winds from the QuikSCAT satellite and its effects on the geneses of tropical cyclones in the South China Sea. *Tellus A*, **59**: 562-569.

Webster, P. J., Holland, G. J., Curry, J. A., and Chang, H. R., 2005. Changes in tropical cyclone number, duration, and intensity in a warming environment. *Science*, **309**: 1844-1846.

Webster, P. J., Curry, J. A., Liu, J., and Holland, G. J., 2006. Response to comment on 'Changes in tropical cyclone number, duration, and intensity in a warming environment'. *Science*, **311**: 1713c.

Wu, B., and Zhou, T. J., 2008. Oceanic origin of the interannual and interdecadal variability of the summertime western Pacific subtropical high. *Geophysical Research Letters*, **35**, L13701, DOI: 10.1029/2008GL034584.

Wu, L. G., and Wang, B., 2004. Assessing impacts of global warming on tropical cyclone tracks. *Journal of Climate*, **17**: 1686-1698.

Wu, L. G., Wang, B., and Geng, S. Q., 2005. Growing typhoon influence on East Asia. *Geophysical Research Letters*, **32**, L18703, DOI: 10.1029/2005GL022937.

Yumoto, M., and Matsuura, T., 2001. Interdecadal variability of tropical cyclone activity in the Western North Pacific. *Journal o f the Meteorological Society of Japan*, **79**: 23-35.

Zhang, Y., Wallace, J. M., and Battisti, D. S., 1997. ENSO-like interdecadal variability: 1900–93. *Journal of Climate*, **10**, 1004-1020.

Zhou, T., Yu, R., Zhang, J., Drange, H., Cassou, C., Deser, C., Hodson, D. L. R., Sanchez-Gomez, E., Li, J., Keenlyside, N., Xin, X., and Okumura, Y., 2009. Why the western Pacific subtropical high has extended westward since the Late 1970s. *Journal of Climate*, **22**: 2199-2215.

Zuki, Z. M., and Lupo, A. R., 2008. Interannual variability of tropical cyclone activity in the southern South China Sea. *Journal of Geophysical Research*, **113**: D06106, DOI: 10.1029/2007JD009218.

(Edited by Xie Jun)